RSC Advances

ROYAL SOCIETY OF CHEMISTRY

www.rsc.org/advances

Journal Name

RSCPublishing

ARTICLE

Preparation and characterization of polyurethane-imide/ kaolinite nanocomposite foams

Xinggang Chen,[a,b] Xiaoming Sang*[b] and Qingxin Zhang*[a]

Cite this: DOI: 10.1039/xoxxoooooox

Received ooth January 2012,
Accepted ooth January 2012

DOI: 10.1039/xoxxoooooox

www.rsc.org/

A novel polymer/kaolinite nanocomposite based on polyurethane-imide (PUI) foams was prepared by *in-situ* polymerization. The PUI foams were synthesized via the reaction between isocyanate terminated polyimide prepolymers and polyether polyol. The kaolinite was modified with the intercalating agent of potassium carbonate. XRD analyses of the intercalated kaolinite and the PUI/kaolinite nanocomposite foams indicate that both intercalated and exfoliated structures are formed. The cell structure, cell size distribution, thermal stability and mechanical properties of the PUI/kaolinite nanocomposite foams are characterized by SEM, TG and electronic universal testing method. Kinetics of thermal degradation and thermal aging life of the nanocomposite foams are investigated and forecasted compared with those of the pure PUI foams. The results show that addition of the kaolinite significantly improves the heat resistance and mechanical properties. However, the functional groups of PUI foams don't change obviously.

Introduction

Polyurethane-imide (PUI) foams, a new member of high performance foams, have attracted considerable attention in recent years.[1-3] The main chain of PUI not only contains the polyurethane with soft and hard segments, but also includes the polyimide with nitrogen heterocycles, which inherit the advantages of both polyimide foams and polyurethane foams, such as good resistance to high temperature, thermal insulation properties, and sound absorption properties, etc.[4-6] As a kind of foam core sandwich materials, PUI foams are widely used in aerospace, marine, military and other fields. However, due to the increasing concern for the high-performance foams in some special areas, it is urgently necessary to further improve the properties of PUI foams, particularly the thermal stability and mechanical properties.

In recent years, polymer/layered silicate nanocomposites have attracted great interests, both in industry and academic fields. Generally, the larger the surface of the filler in contact with the polymer, the greater the reinforcing effect will be. Silicate layers are two-dimensional nano materials with an extremely high specific surface area. And the strong interactions between the polymer and the layered silicate lead to dispersion of the organic and inorganic phases at the nanometer level. Therefore, layered silicates impart obvious improvements of mechanical properties even when employed at very low loading in a polymer matrix. Furtherly, layered silicates act as a superior insulator and mass transport barrier to the volatile products generated during decomposition, which enhances the thermal stability of the polymer matrix. Of course, in addition, polymer/layered silicate nanocomposites frequently exhibit other unexpected unique properties compared with virgin polymer, such as electrical conductivity and gas barrier property, without significant reductions in toughness and transparency. Layered silicate nanoclay is a good candidate due to the abilities which make the cell sizes of the foam smaller as a bubble nucleating agent and reduce the gas diffusion as diffusion barriers. Among the layered silicate nanoclay, the commonly studied nanocaly are attapulgite,[7-9] rectorite,[10] saponite,[11] sepiolite,[12,13] montmorillonite (MMT),[14-19] kaolinite[20-25] and so on. Among them, the most widely utilized clay is montmorillonite due to its large cation exchange capacity. Thus, polymer/layered silicate nanocomposite foams have been mainly reported with montmorillonite. However, kaolinite, as a kind of promising materials, has attracted great interests. Recently kaolinite has been used in many types of composite foam, including starch foams[26], NR foams[27], polyurethane-polyisocyanurate foams[28], polyurethane foams[29], poly (methyl methacrylate)/poly (urethane-urea) foams[30], and so on. The involvement of the kaolinite increases the compression modulus, compression strength, izod impact strength, thermal resistance, water absorption capability, and nonflammability of the nanocomposite foams. Moreover, uniform cell size distribution of the nanocomposite foams is also obtained.

Kaolinite is an aluminosilicate with an ideal composition of $Al_2Si_2O_5(OH)_4$, which is a mineral of 1:1 phyllosilicate and composed of interstratified $AlO_2(OH)_4$ octahedral and SiO_4 tetrahedral sheets.[31] The interlayer space is unsymmetrical,

which leads to the formation of hydrogen bonds between consecutive layers, providing a large cohesive energy. Moreover, kaolinite is neutral and no ions exist in the gallery space, which also prevents the insertion of substances into the interlamellar space. Therefore, only small and highly polar molecules can directly intercalate into the interlayer of kaolinite, such as dimethylsulfoxide (DMSO), deuterated dimethylsulfoxide, formamide, N-methylformamide, imethylformamide, acetamide, pyridine N-oxide, potassium acetate, methanol and octadecylamine.[32-39] Then the materials with higher molecular weight tend to insert into the interlayer of kaolinite by replacing these small molecules.

In this work, new nanocomposites prepared from PUI foams and kaolinite were reported, and the main objective was to obtain a kind of new nanocomposite foams with enhanced thermal stability and mechanical properties. The cell morphology (cell structure, cell size distribution), mechanical properties, thermal properties, kinetics of thermal degradation and thermal aging life of the PUI/Kaolinite nanocomposite foams were also investigated as a function of composition.

2 Experimental

2.1 Materials

3,3-4,4-benzophenonetetracarboxylic dianhydride (BTDA) from Beijing Multi. Technology Co. Ltd. (Priority level, 99.5 wt.%) was purified by recrystallization from acetic anhydride and then dried in a vacuum oven at 125 ^{o}C overnight. Polyether polyol from Nanjing Chen Han Polyurethane Co. Ltd (Hydroxyl value (KOH mg/g): 430±30, water (wt.%): ≤ 0.15, PH value: 9.0~11.0) was dried in a vacuum oven at 100 ^{o}C overnight. Polymeric diphenylmethane diisocyanate (PM-200) was obtained from Yantai Wanhua Polyurethanes Co. Ltd (-NCO%: 30.2~32.0, Density (25 ^{o}C, g/cm^{3}): 1.22 ~ 1.25, Acid Content (HCl)%: ≤ 0.05, Hydrolyzable Chlorine% ≤ 0.2). Kaolinite was provided by China sinoma Co. Ltd (SiO_2 46.65 wt.%, Al_2O_3 36.14 wt.%, Fe_2O_3 0.19 wt.%, TiO_2 0.14 wt.%, CaO 0.31 wt.%, MgO 0.43 wt.%, K_2O 0.16 wt.%, Na_2O 0.27 wt.%, I.L 13.68 wt.%). Other reagents and solvents were obtained commercially and then used as received without further purification.

2.2 Preparation of Intercalated Kaolinite

The original kaolinite with the mass of 5 g was transferred to a mortar and suspended in 10 g of potassium acetate. In the condition of natural deliquescent, the mixtures were ground for 3 days, washed with plenty of deionized water to completely remove excessive potassium acetate, and then oven-dried at 60 ^{o}C for 12 h.

2.3 Synthesis of isocyanate terminated polyimide prepolymers

Two gram of BTDA, preliminarily dissolved in 10 mL of N, N-dimethyl formamide (DMF), was added into a 250-mL four-necked flask, fitted with a mechanical stirrer, a reflux condenser and a N_2 inlet and outlet. After the BTDA was fully dissolved, the mixture was slowly heated to 60 ^{o}C in an oil bath. Then 14 g of PM-200 was added into the BTDA solution and maintained at 60 ^{o}C for 1 h. After that, the mixture was heated to 120 ^{o}C and kept for 3 h in order to obtain the imide heterocyclic structure. Afterwards, polyimide prepolymer samples were set aside for further usage.

2.4 Preparation of PUI/kaolinite nanocomposite foams

The polyether polyol with the mass of 10 g was added into a plastic cup, following by addition of distilled water (0.2 g), n-pentane (0.9 g), triethanolamine (0.024 g), stannous octoate (0.1 g), dimethyl silicone oil (0.4 g) and ethylene glycol monomethyl ether (0.3 g) at the meantime. Then the mixture was stirred until the system had a certain viscosity, which were named as component *A* and then allowed to standby. The intercalated kaolinites with different percentage (1 wt.%, 3 wt.%, 5 wt.%, 7 wt.% and 9 wt.%) were added into isocyanate terminated polyimide prepolymers with stirring and the mixture was heated at 80 ^{o}C in an oil bath for 30 min, followed by sonication using an ultrasonic cell crusher instrument for 30 min, which were named as component *B* and allowed to standby. In the following step, component *A* was mixed with component *B* at the speed of 3000 rpm for 10 s and then the resulted reaction mixture were quickly poured into an open Teflon mold. After demoulding, the nanocomposite foams were placed in a vacuum oven at 80 ^{o}C for 24 h and cured at room temperature for another 24 h. The core bodies of nanocomposite foams were used as test samples for further characterization.

2.5 Characterization

To determine the basal spacing of the clays, X-ray diffraction (XRD) was carried out at ambient temperature on a D/MAX2500PC diffractometer (RIGAKU, Japan) with Cu (λ=1.54178 Å) irradiation at the scanning rate of 2 °/min in the 2θ range of 5~30 °. Fourier transform infrared spectra of intercalated kaolinite and PUI/kaolinite nanocomposite foams were recorded by a VATAR380 FTIR spectrometer (NICOLET, USA) with a resolution of 2 cm^{-1} from 4000 cm^{-1} to 400 cm^{-1} using KBr pellets. The nanocomposite foam density was determined indirectly by the drainage volume method, and calculated via dividing the weight by the measured volume of rectangular shaped samples. The apparent density was determined from the average of at least three samples. Compression properties were carried out on AGS-X electronic tensile tester (SHIMADZU, Japan) with a crosshead speed of 10mm/min after samples were made into 50×50×50 mm. The cellular structure was performed with S-4800 scan electron microscope (SEM, HITACHI, Japan) using an acceleration of 20 kV. Samples were made into 1×1×1 mm and platted gold by ion sputtering. The images were analyzed by Adobe Photoshop 8.0 and Image Pro Plus 6.0 software. At minimum of 20 pores per foam were manually traced and used in the image analysis. The thermogravimetric analysis of nanocomposite foams was performed on a TG-DTA Analyzer STA449 thermal analyzer (NETZSCH, German) a temperature range of 50~800 ^{o}C under N_2 atmosphere at different heating rates (10, 15 and 20 ^{o}C/min).

3 Results and discussion

3.1 XRD analysis of intercalated kaolinite

Fig.1 shows the XRD patterns of original kaolinite (**Kao**) and intercalated kaolinite with potassium acetate (**Kao-KAc**). It can be observed from Fig.1 that the 2θ value of d (001) peaks of **Kao** appears at 12.36 °, while that of **Kao-KAc** is at 6.28 °, which is the same as that reported by Essawy[34]. Moreover, the basal d (001) of kaolinite expands from 0.72 to 1.41 nm, with an increase of 0.69 nm, which indicates the intercalation of

Kao-KAc in the interlamellar space and large expansions in the kaolinite structure caused by potassium acetate. Meanwhile, it can be obtained that the intercalation ratio of **Kao-KAc** with potassium acetate is of 86.71 wt.%, calculated from the integrated areas of the reflections.

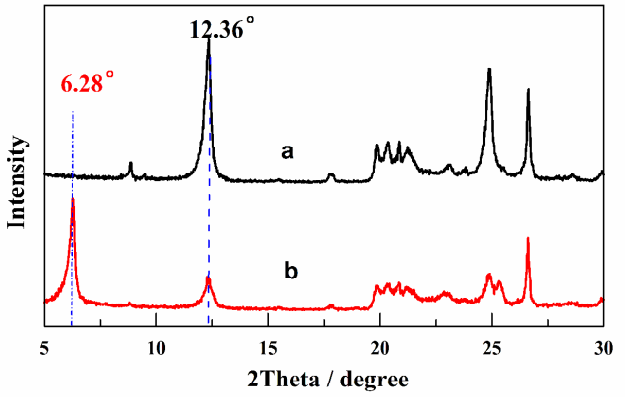

Fig.1 XRD patterns of (a) **Kao** and (b) **Kao-KAc**

3.2 XRD analysis of PUI/Kaolinite nanocomposite foams

XRD patterns of nanocomposite foams are exhibited in Fig.2 to study the exfoliation of kaolinite in the foam matrix.

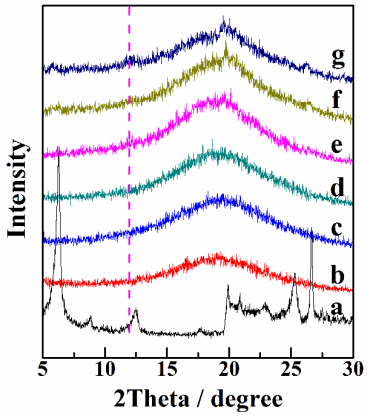

Fig.2 XRD patterns of PUI/Kaolinite nanocomposite foams: (a) pure **Kao-KAc**, (b) pure PUI foams, (c) 1 wt.% **Kao-KAc**, (d) 3 wt.% **Kao-KAc**, (e) 5 wt.% **Kao-KAc**, (f) 7 wt.% **Kao-KAc**, (g) 9 wt.% **Kao-KAc**

As seen from Fig.2, basal d (001) peaks of **Kao-KAc** are at 6.28 ° and 12.35 ° in curve (a), while no diffraction peaks are observed for pure PUI foams as shown in curve (b). When low contents of **Kao-KAc** are added into PUI foams, d (001) peaks at 6.28 ° and 12.35 ° are not observed in curve(c-e), indicating that the **Kao-KAc** are well exfoliated and dispersed in PUI foam matrix.[31] The basal d (001) peaks at 12.35 ° begin to appear with 7 wt.% of **Kao-KAc** and then become apparent with Kao-KAc content increasing to 9 wt.%. The results indicate that potassium acetate escapes from kaolinite layers with increased content, which may be due to the heating and the agglomeration of the kaolinite in the PUI foam matrix.

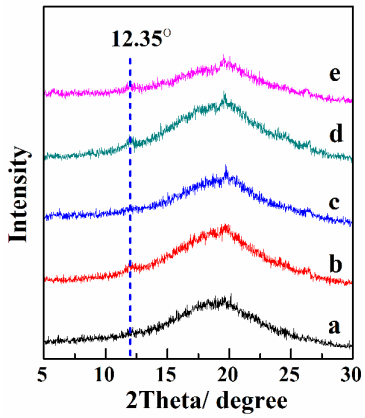

Fig.3 XRD patterns of PUI/ kaolinite nanocomposite foams: (a) 5 wt.% **Kao-KAc**, (b) 5 wt.% **Kao**, (c) 7 wt.% **Kao-KAc**, (d) 7 wt.% **Kao**, (e) 9 wt.% **Kao-KAc**

Fig.3 shows the XRD comparison chart of **Kao-KAc** and **Kao** in PUI foams. It can be seen that d(001) peak at 12.35 ° appears when the loading of **Kao** is 5 wt.%. Compared with those of **Kao**, there are tiny peaks at 12.35 ° when the loading of **Kao-KAc** is 9 wt.%, with intensity of the d (001) peak still weaker than that when the loading of **Kao** is 5 wt.%. The results indicate that **Kao-KAc** not only effectively promotes the exfoliation of kaolinite, but also avoids the agglomeration of kaolinite in PUI foam matrix.

3.3 Cell structure and cell size distribution of nanocomposite foams

The size of closed cells and the distribution of cell sizes are important parameters for various performances.[40-42] Typical porous cell diameters are obtained by inspecting visually the diameter of at least 20 porous cells on the surface of nanocomposite foams. Fig.4 shows the SEM morphologies and cell size distribution of PUI nanocomposite foams with different contents of intercalated kaolinite. The cell size distribution is strongly influenced by the content of intercalated kaolinite. There is a wide range of diameter distribution in nanocomposite foams when the loading of intercalated kaolinite are 1 wt.%, 3 wt.% and 9 wt.%, respectively. When the loading of intercalated kaolinite is 5 wt.%, the mean cell size is mainly in the range of 0.6~0.7 mm, with that in range of 0.7~0.9 mm when the loading is 7 wt.%. These two distributions are more narrow and uniform than those of other nanocomposite foams.

Fig.5 presents mean cell sizes of PUI/kaolinite nanocomposite foams with different contents of intercalated kaolinite. It can be seen that the mean cell size of nanocomposite foams decreases firstly and then increases with increased contents of intercalated kaolinite. When the content of intercalated kaolinite is of 5 wt.%, the mean cell size reaches the minimum value (0.70 mm). As the content further increasing to 7 wt.% and 9 wt.%, the mean cell sizes increase to 0.83 and 0.93 mm, respectively. However, these values are still lower than those of pure PUI foams. The possible reason is that intercalated kaolinite seems to slightly restrict the expansion of foam by slowing down desorption rate of CO_2 from PUI foam, especially the exfoliated kaolinite. On the other side, it is believed that the exfoliated kaolinite acts as an effective heterogeneous nucleating agent, leading to the increase of the closed cells number. Nevertheless, with the content of intercalated kaolinite increasing, the obvious agglomeration easily occurs in the process of preparation and decreases the benefit of heterogeneous nucleation, resulting in the increase of cell sizes.

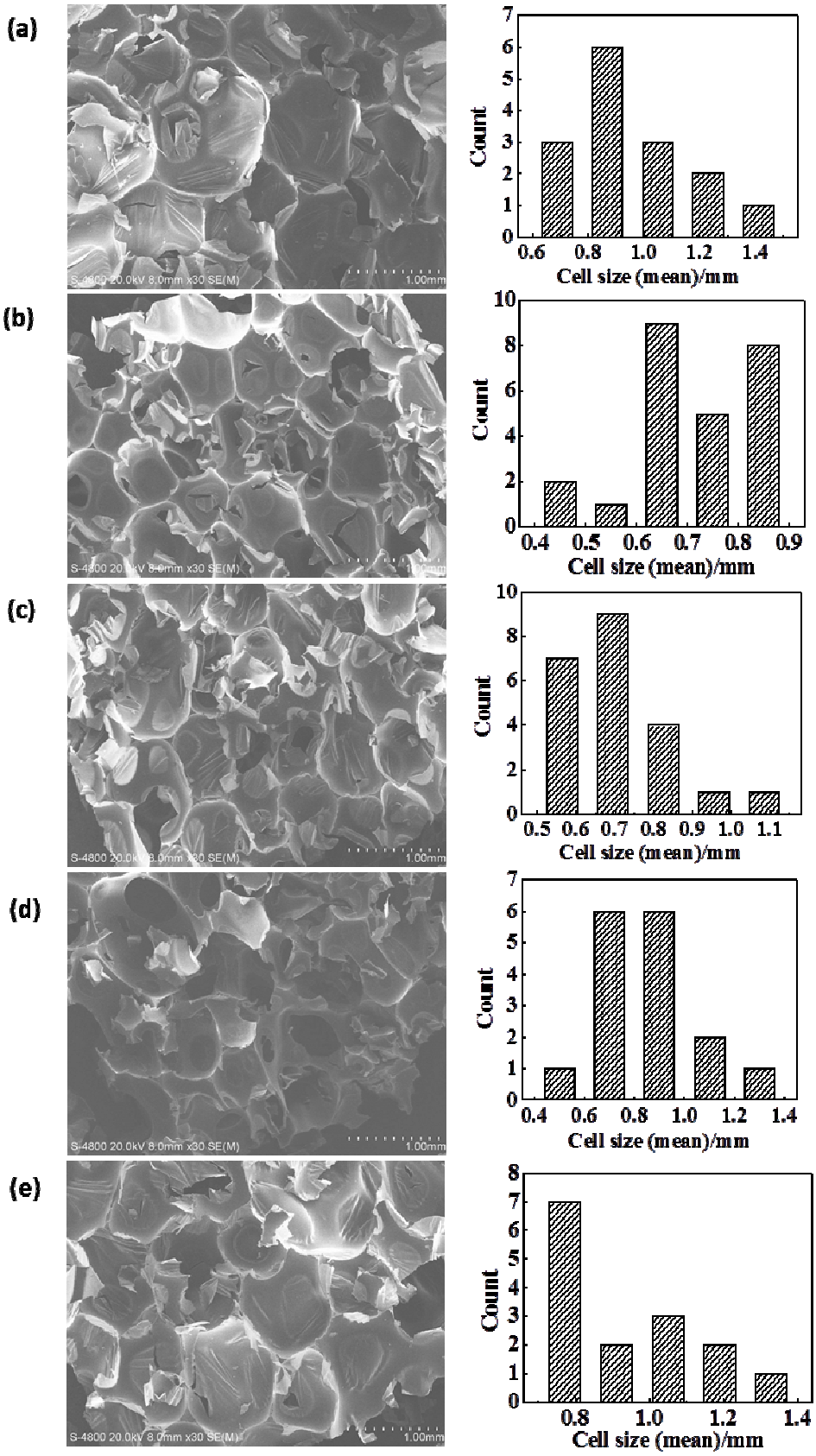

Fig.4 SEM micrographs and cell size distributions of PUI/kaolinite nanocomposite foams: (a) 1 wt.% **Kao-KAc**, (b) 3 wt.% **Kao-KAc**, (c) 5 wt.% **Kao-KAc**, (d) 7 wt.% **Kao-KAc**, (e) 9 wt.% **Kao-KAc**

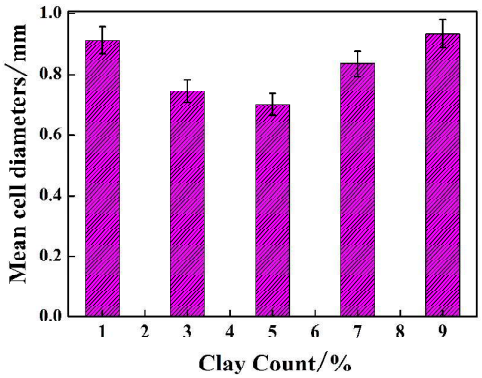

Fig.5 Mean cell sizes of PUI/kaolinite nanocomposite foams

3.4 Density and mechanical properties

Density is the most important parameter in order to control the mechanical property of foams.[43] Table 1 shows the effect of density and compressive properties with different contents of intercalated kaolinite compared with those of the pure PUI foams. The introduction of intercalated kaolinite to PUI foams makes the density increase from 41.03 to 80.85 kg/m^3, which may be caused by following two factors. On one hand, the increasing viscosity of the overall material system can hinder the foaming process, which results in higher density foam. On the other hand, as a heterogeneous nucleating agent, intercalated kaolinite increases the number of closed cells, which also leads to higher density foam.

As seen from Table 1, the addition of intercalated kaolinite improves the yield strength, compression strength and compression modulus of PUI foams. When the loading is 5 wt.%, the yield strength and compressive strength of nanocomposite foams are the best, 0.18 and 0.19 MPa, respectively. There also exists a maximum compression modulus of nanocomposite foams, 3.58 MPa, when the loading is 7 wt.%. However, the strength and modulus of nanocomposite foams decrease with the content of intercalated kaolinite increasing continually.

Table 1 Densities and Compression properties of PUI/kaolinite nanocomposite foams

Kao-KAc Content /wt.%	Apparent density /(kg•m^{-3})	Yield Strength /MPa	Compressive strength /MPa	Yong's modulus /MPa
0	41.03	0.08	0.11	1.77
1	54.63	0.09	0.12	1.77
3	68.69	0.11	0.13	2.16
5	70.79	0.18	0.20	3.33
7	72.50	0.17	0.17	3.58
9	80.85	0.13	0.17	2.61

The results indicate that kaolinite interlayers play an important role in cross-linking points of PUI foams with a large specific surface area and interfacial interaction, which increases the strength and modulus of PUI foams. Although the increase in the apparent density of nanocomposite foams is beneficial to mechanical properties, the possibility of the agglomeration of kaolinite is likely to grow when the addition of intercalated kaolinite is excessive, especially in the circumstances with a highly viscous material system, resulting in the bad dispersibility and compatibility of the kaolinite in PUI foams matrix.

3.5 Thermal properties of nanocomposite foams

Thermogravimetric analysis. Fig.6 shows the TG curves of PUI/kaolinite nanocomposite foams. It can be seen that all of PUI/kaolinite foams have three stages during the thermal degradation process. The first degradation stage is at the temperature range of 150~295 °C, which is mainly due to the evolution of CO_2 caused by the partial imidization reaction. The second degradation stage is at the temperature range of 295~390 °C, during which period the soft segments in PUI chain begin to decompose. The third degradation stage is at the temperature range of 390~600 °C, which is due to the decomposition of hard segments in PUI chain. The characteristic data of thermal analysis for PUI/kaolinite nanocomposite foams are summarized in Table 2. As shown from Table 2, the increase of intercalated kaolinite enhances the decomposition temperatures, and the char yields at 800 °C are 20.6 %, 27.04 % and 30.81 %, respectively. The results show that thermal stability of PUI/kaolinite nanocomposite foams significantly improves with the increase of the loading of intercalated kaolinite.

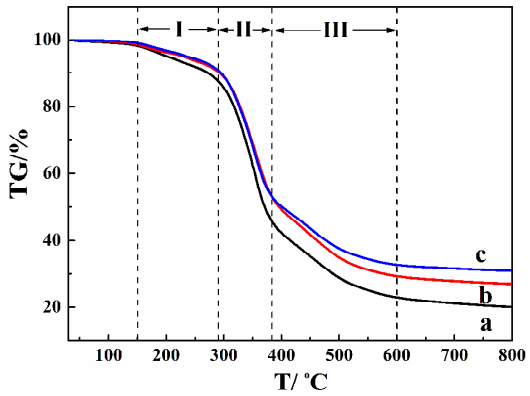

Fig.6 TG curves of PUI/kaolinite nanocomposite foams: (a) 1 wt.% **Kao-KAc**, (b) 5 wt.% **Kao-KAc**, (c) 7 wt.% **Kao-KAc**

Table 2 Thermal analyses of PUI/kaolinite nanocomposite foams

Kao-KAc Content /wt.%	$Td_{5\%}$ / °C	$Td_{10\%}$ / °C	$Td_{50\%}$ / °C	Char yield at 800 °C/%
1	202	272	372	20.60
5	230	292	396	27.04
7	238	296	402	30.81

Kinetics of the thermal degradation. The application of dynamic TG methods holds great promise as a tool for unravelling the mechanisms of physical and chemical processes, which occur during polymer degradation process. To evaluate the thermal stability detailly, non-isothermal thermal degradation kinetics were calculated[44-47]. Kissinger method, as the most widely used method for kinetic, is used to study the thermal properties of

PUI/kaolinite nanocomposite foams and the principle is shown in Eq.(1):

$$\ln\left(\frac{\beta_i}{T^2_{p_i}}\right) = \ln\frac{A_k R}{E_k} - \frac{E_k}{R}\frac{1}{T_{p_i}} \quad (i = 1,\ 2,\ 3) \qquad (1)$$

Where β_i is the heating rate (K·s^{-1}), A_k is the pre-exponential factor (s^{-1}), R is the gas constant (J·kg^{-1}·mol^{-1}·K^{-1}), E_k is the activation energy for composite thermal degradation (J mol^{-1}), and T_{p_i} is the temperature that occurs at the maximum rate (K). Kissinger assumes that α value, defined as the conversion degree (%), is approximately equal for different β_i values at T_{p_i} where d(dα/dt)/dt is zero. E_k and A_k can be calculated from $\ln(\beta_i/T^2_{p_i})$ versus $1/T_{p_i}$ plot for different conversion degrees.

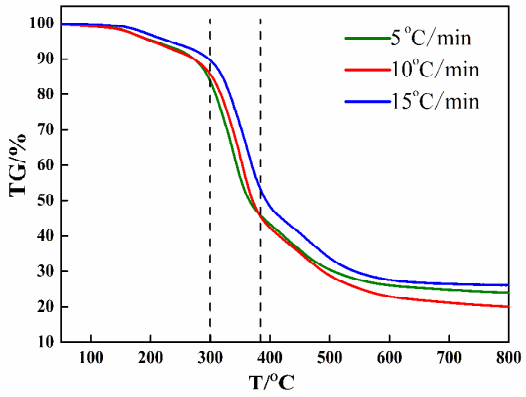

Fig.7 TG curves of PUI/kaolinite nanocomposite foams with 5 wt.% of **Kao-KAc** at different heating rates

Table 3 Kinetic data of thermal degradation of PUI/kaolinite nanocomposite foams

Conversion, α / wt.%	Activation energy, E_k / (kJ·mol^{-1})	Pre-exponential factor, A_k / (s^{-1})
0.649	90.862	144.772
0.617	88.506	109.350
0.585	88.007	115.010
0.552	86.942	105.572
0.520	85.967	97.505
0.488	85.791	105.584
0.456	85.817	119.304
0.423	85.369	122.827
0.391	84.495	116.692
0.359	83.498	108.841
0.327	82.388	99.525
0.294	80.965	85.360
0.262	79.037	66.215
Mean	E_k=84.92 kJ/mol	A_k=107.62 s^{-1}

Fig.7 shows the TG curves of PUI/kaolinite nanocomposite foams with 5 wt.% of KAc. To meet the requirements of Kissinger method, different heating rates of 5, 10 and 15 °C/min are used for the isoconversional analysis.

It is generally observed from Fig.7 that there also exist three stages during the thermal degradation process. Since soft segments of PUI have worse thermal properties than the hard segments, they are picked up to stand for PUI/kaolinite nanocomposite foams at the second degradation stage. As can be derived from Fig.7, the practical degradation temperature of soft segments is in the range of 300~380 °C, which are divided into fifteen equal portions. Hence, a set of α values (0.649, 0.617, 0.585, 0.552, 0.520, 0.488, 0.456, 0.423, 0.391, 0.359, 0.327, 0.294 and 0.262) are taken. Then T values are calculated by the linear regression method corresponding to certain α value, and the corresponding E_k and A_k can be obtained from Kissinger method for each α value, as shown in Table 3.

Forecast of thermal aging life. According to thermal aging life of organic polymer materials, many empirical formulas have been established. Dakin empirical formula is chosen to investigate the thermal aging life of PUI/kaolinite nanocomposite foams, as shown in Eq.(2)[48]:

$$\lg\tau = a\frac{1}{T} + b \qquad (2)$$

Where τ is the life of the polymer material at the temperature T, and a, b are both constants.

Thermal degradation reaction equation is given in Eq. (3):

$$-\frac{d\alpha}{dt} = A_k\alpha^n \exp\left(\frac{-E_k}{RT}\right) \qquad (3)$$

Where $d\alpha/dt$ is the isothermal rate of conversion, α is the percentage of residual mass and n is the order of the reaction. Eq. (4) is obtained by integrating of Eq. (3), as follows:

$$\int_1^{\alpha_\tau} -\frac{d\alpha}{\alpha^n} = A\exp\left(\frac{-E}{RT}\right)\int_0^T dt \qquad (4)$$

Where α_τ is the percentage of residual mass of end lives.

According to Kissinger's peak shape index (S), three tangents are drawn for the peak of the thermal decomposition in DTA curve, and the meaning of S is the ratio of the distance a and b, that is S = a / b, as shown in Fig.8. The order of the reaction is obtained directly based on the relationship between n and S, as follows:

$$n = 1.26 \times S^{1/2} \qquad (5)$$

According to Eq. (5), the reaction order of thermal decomposition reactions is 1.14 in the soft section of PUI foams. Therefore, n is approximately evaluated to an integer (n=1) in the following calculation.

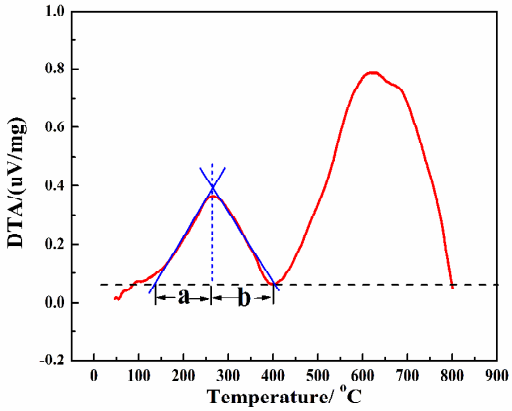

Fig.8 DTA curve of PUI/kaolinite nanocomposite foams

The logarithm of τ based on Eq. (4) is obtained directly.

$$\lg \tau = \frac{E}{2.303}\frac{1}{RT} + \lg\left(-\frac{\ln \alpha_\tau}{A}\right) \quad (6)$$

The following equation can be obtained by the calculation of Eq. (2) and Eq. (6),

$$a = \frac{E}{2.303R} \qquad b = \lg(-\frac{\ln\alpha_\tau}{A}) \quad (7)$$

E_k and A_k are respectively obtained from the results calculated in Table 2. Where 15 wt.% is defined as the indicator of end life, the values of a and b are obtained.

$$a = 4435.07 \qquad b = -2.82 \quad (8)$$

The life curve of kaolinite/ polyurethane-imide foams at 15 wt.% is obtained by plotting T against τ, as shown in Fig.9.

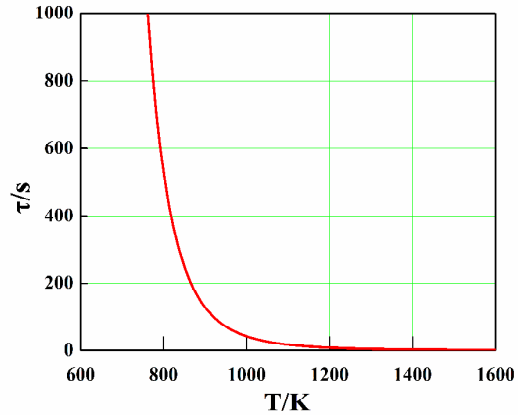

Fig.9 Life curve of PUI/kaolinite nanocomposite foams at 15 wt.% weight loss

As can be seen from Fig.9, the thermal aging life τ and the limit temperature T can be estimated at some extent. The data in Table 4 represent the estimated using lives of PUI/kaolinite at different temperatures (100, 200, 300 and 400 °C). It shows that the upper limit of use temperature of nanocomposite foams should be below 200 °C.

Table 4 Estimated using lives of PUI/kaolinite nanocomposite foams

Temperature / °C	Life / h
400	1.40
300	20.83
200	540.00
100	164192.45

3.6 Chemical structure of nanocomposite foams

Fig.10 represents the FTIR spectra of PUI/kaolinite nanocomposite foams with different contents of **Kao-KAc**. As shown in Fig.10, the absorption band at 1728 cm^{-1} is related to C=O stretching vibration in the imide chain. The absorption bands at 1619, 1525, 1232 and 1098 cm^{-1} represent N-H bending vibration peak, C=O stretching vibration peak, C-N stretching vibration peak and C-O bending vibration peak in the urethane chain, respectively. The absorption bands at 2960 and 815 cm^{-1} represent C-H stretching vibration peak and C-H bending vibration peak. The major peaks of pure PUI foams are the same as that of PUI/kaolinite nanocomposite foams, indicating that the addition of kaolinite does not change the chemical structures of PUI/kaolinite nanocomposite foams.

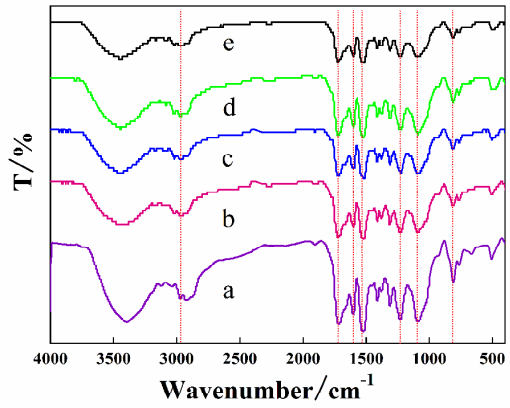

Fig.10 FTIR spectra of PUI/kaolinite nanocomposite foams: (a) 0 wt.% **Kao-KAc**, (b) 1wt.% **Kao-KAc**, (c) 3 wt.% **Kao-KAc**, (d) 5 wt.% **Kao-KAc**, (e) 7 wt.% **Kao-KAc**

4 Conclusions

In this work, foams of new PUI/kaolinite nanocomposites were prepared by *in-situ* polymerization. XRD analyses show that potassium acetate is successfully intercalated into the layers of kaolinite. The amount of intercalated kaolinite in PUI foams has a great influence on the exfoliation and dispersion of kaolinite in the PUI foams. With the increase of intercalated kaolinite, the mean cell size of PUI foams first decreases and then increases. On the contrary, mechanical properties of PUI/kaolinite nanocomposite foams first increase and then decrease. Nevertheless, excessive amounts will lead to the obvious agglomeration of kaolinite, resulting in the poor exfoliation and dispersion in the matrix, the increase of cell sizes and the decrease of mechanical properties. As a heterogeneous nucleating agent, the addition of kaolinite effectively increases the density and improves thermal stability of nanocomposite foams. According to kinetics of the thermal degradation and the forecast of thermal aging life, the limiting temperature of nanocomposite foams should be below 200 °C. FTIR tests show that the chemical structures of PUI foams don't change noticeably after the addition of intercalated kaolinite. In consequence, the PUI/Kaolinite nanocomposite foams with excellent mechanical properties, thermal stability and good cell structure have a tremendous potential to be used as the heat-resisting material insulation materials, noise and vibration control of acoustic absorbing material and thermal insulation for building construction.

Acknowledgements

The authors express their thanks to Natural Science Foundation of Hebei Province (E2014209280) and Colleges and universities in Hebei province science and technology key research project (ZH2012014) for financial support.

Notes and references

[a] Institute of Polymer Science and Engineering, School of Chemical Engineering and Technology, Hebei University of Technology, Tianjin 300130, PR China, Email: zhqxcn@163.com

[b] Hebei Province Key Laboratory of Inorganic Nonmetallic Materials, School of Materials Science and Engineering, North China University of

Science and Technology, Tangshan Hebei 063009, PR China, Email: xmsang2007@163.com

1. C. F. Zhou, J. M. Gou, and T. Zhai, *New. Mat. Chem.*, 2005, **33**, 24-25.
2. X. M. Sang, X. G. Chen, G. X. Hou and S. W. Yu, *Adv. Mater. Res.*, 2011, **150**, 1123-1126.
3. Q. Tang, Y. Song, J. He and R. Yang, *J. Appl. Polym. Sci.*, 2014, 131.
4. A. Avcı and K. Şirin, *Des. Monomers. Polym.*, 2014, **17**, 380-389.
5. Q. Tang, Q. Ai, J. He, X. Li and R. Yang, *High Perform. Polym.*, 2013, 0954008313486280.
6. M.H. Park, W. Jang, S.J. Yang, Y. Shul and H. Han, *J. Appl. Polym. Sci.*, 2006, **100**, 113-123.
7. Y. Zheng, J. Zhang and A. Wang, *Chem. Eng. J.*, 2009, **155**, 215-222.
8. H. Yin, H. Chen and D. Chen, *Colloid. Surface. A*, 2010, **367**, 52-59.
9. L. Wang and J. Sheng, *Polymer*, 2005, **46**, 6243-6249.
10. W. Wang and A. Wang, *Carbohyd. Polym.*, 2009, **77**, 891-897.
11. J.-M. Yeh and K.-C. Chang, *J. Ind. Eng. Chem.*, 2008, **14**, 275-291.
12. D. García-López, J. F. Fernández, J. C. Merino, J. Santarén and J. M. Pastor, *Compos. Sci. Technol.*, 2010, **70**, 1429-1436.
13. H. Chen, D. Zeng, X. Xiao, M. Zheng, C. Ke and Y. Li, *Mat. Sci. Eng. A-Struct*, 2011, **528**, 1656-1661.
14. X. Zhang, G. Lin, R. Abou-Hussein, M. K. Hassan, I. Noda and J. E. Mark, *Eur. Polym. J.,* 2007, 43, 3128-3135.
15. C. Yang, Y. Dingyang, Z. Huawei and L. Mei, *RSC Adv.*, 2014, **4**, 44750-44756.
16. U. Riaz, S. A. Ahmad, S. Ahmad and S. M. Ashraf, *Polym. Composite.*, 2010, **31**, 906-912.
17. E. S. Jang, S. B. Khan, J. Seo, Y. H. Nam, W. J. Choi, K. Akhtar and H. Han, *Prog. Org. Coat.*, 2011, **71**, 36-42.
18. R. Das, R. Kumar, S. L. Banerjee and P. P. Kundu, *RSC Adv.*, 2014, **4**, 59265-59274.
19. K. Chrissopoulou and S. H. Anastasiadis, *Eur. Polym. J.,* 2011, **47**, 600-613.
20. X. Zhao, B. Wang and J. Li, *J. Appl. Polym. Sci.*, 2008, **108**, 2833-2839.
21. L. Wang, X. Xie, S. Su, J. Feng and C. A. Wilkie, *Polym. Degrad. Stabil.*, 2010, **95**, 572-578.
22. D. Sun, Y. Li, B. Zhang and X. Pan, *Compos. Sci. Technol.*, 2010, **70**, 981-988.
23. M. H. A. Rehim, A. M. Youssef and H. A. Essawy, *Mater. Chem. Phys.*, 2010, **119**, 546-552.
24. J. Matusik, E. Stodolak and K. Bahranowski, *Appl. Clay Sci.*, 2011, **51**, 102-109.
25. S. Letaief and C. Detellier, *Langmuir*, 2009, **25**, 10975-10979.
26. K. Kaewtatip, V. Tanrattanakul and W. Phetrat, *Appl. Clay Sci.*, 2013, **80**, 413-416.
27. N. Tangboriboon, S. Samattai, J. Kamonsawas and A. Sirivat, *Mater. Manuf. Process.*, 2015, **30**, 595-604.
28. J. Liszkowska, B. Czupryński and J. Paciorek-Sadowska, *J. Cell. Plast.*, 2013, **49**, 375-390.
29. M. Dalen, A. Ibrahim, H. Adamu and A. Nurudeen, *Int. Res. J. Pure Appl. Chem.*, 2014, **4**, 691-709.
30. A. Kausar, *J. Compos. Mater.*, 2014, **0**, 1-10.
31. S. Pavlidou and C. D. Papaspyrides, *Prog. Polym. Sci.*, 2008, **33**, 1119-1198.
32. H. Cheng, Q. Liu, J. Yang, Q. Zhang and R. L. Frost, *Thermochim. Acta.*, 2010, **503-504**, 16-20.
33. T. A. Elbokl and C. Detellier, *J. Colloid. Interf. Sci.*, 2008, **323**, 338-348.
34. H. A. Essawy, A. M. Youssef, A. A. Abd El-Hakim and A. M. Rabie, *Polym-Plast. Technol.*, 2009, **48**, 177-184.
35. S. Letaief, T. A. Elbokl and C. Detellier, *J. Colloid. Interf. Sci.*, 2006, **302**, 254-258.
36. Q. Qiao, H. Yang, J. L. Liu, S. P. Zhao and X. M. Ren, *Dalton T.*, 2014, **43**, 5427-5434.
37. D. Sun, B. Li, Y. Li, C. Yu, B. Zhang and H. Fei, *Mater. Res. Bull.*, 2011, **46**, 101-104.
38. A. Taborosi, R. Kurdi and R. K. Szilagyi, *Phys. Chem. Chem. Phys.*, 2014, **16**, 25830-25839.
39. H. Xu, M. Wang, Q. Liu, D. Chen, H. Wang, K. Yang, H. Lu, R. Zhang and S. Guan, *J Phys. Chem. Solids.*, 2011, **72**, 24-28.
40. L. Urbanczyk, C. Calberg, C. Detrembleur, C. Jérôme and M. Alexandre, *Polymer*, 2010, **51**, 3520-3531.
41. W. Zhai, J. Yu, L. Wu, W. Ma and J. He, *Polymer*, 2006, **47**, 7580-7589.
42. C. Zúñiga, G. Lligadas, J. C. Ronda, M. Galià and V. Cádiz, *Polymer*, 2012, **53**, 3089-3095.
43. Ł. Piszczyk, M. Strankowski, M. Danowska, J. T. Haponiuk and M. Gazda, *Eur. Polym. J.,* 2012, **48**, 1726-1733.
44. S. Bourbigot, J. W. Gilman and C. A. Wilkie, *Polym. Degrad. Stabil.*, 2004, **84**, 483-492.
45. I. B. L. Abate, F. A. Bottino, G. Di Pasquale, E. Fabbri, A. Orestano and a. A. Pollicino, *J. Therm. Anal. Calorim.*, 2008, **91**, 681-686.
46. H. Li and H. Kim, *Desalination*, 2008, **234**, 9-15.
47. Q. Zhou and M. Xanthos, *Polym. Degrad. Stabil.*, 2009, **94**, 327-338.
48. S. M. Manoj Kumar Pradhan, IEEE, and T. S. Ramu, *IEEE T. Poewr Deliver*, 2005, **20**, 1962-1969.

